THE JOURNAL OF PHYSICAL CHEMISTRY B

Article

pubs.acs.org/JPCB

Doping a Mixture of Two Smectogenic Liquid Crystals with Barium Titanate Nanoparticles

Alexander Lorenz,[†,#] Natalie Zimmermann,[†] Satyendra Kumar,[‡] Dean R. Evans,[§] Gary Cook,[∥] Manuel Fernández Martínez,[⊥] and Heinz-S. Kitzerow*[,†]

[†]Department of Chemistry, University of Paderborn, Warburger Str. 100, 33098 Paderborn, Germany

[‡]Department of Physics, Kent State University, Kent, Ohio 44242, United States

[§]Air Force Research Laboratory, Materials and Manufacturing Directorate, Wright-Patterson Air Force Base, Ohio 45433, United States

[∥]Azimuth Corporation, 4134 Linden Avenue, Suite 300, Dayton, Ohio 45432, United States

[⊥]European Synchrotron Radiation Facility, BP220, 38043 Grenoble, France

ABSTRACT: A mixture of two smectic liquid crystals was doped with harvested ferroelectric barium titanate nanoparticles and investigated with wide- and small-angle X-ray scattering during cooling from the isotropic phase. A decrease in the isotropic to nematic and in the nematic to partially bilayer smectic-A_d (SmA_d) phase transition temperatures was observed accompanied by an increase of the layer spacing in the SmA_d phase.

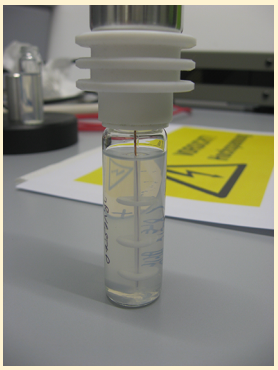

1. INTRODUCTION

The effect of ferroelectric nanoparticles dissolved in liquid crystals (LCs) has been of great scientific interest during the past few years.[1−5] For example, dissolved nanoparticles may give rise to an asymmetry in the electro-optic response of LCs to DC pulses,[1] enhance the optical diffraction efficiency or beam coupling,[2,3] alter the dielectric anisotropy, and shift the phase transition temperatures.[4,5] Recently, it was reported that dispersions of ferroelectric nanoparticles can be prepared by grinding cubic $BaTiO_3$ in heptane with oleic acid as surfactant in a planetary ball mill. This results in a suspension of stressed tetragonal $BaTiO_3$.[6,7] Subsequently, the ferroelectric nanoparticles can be harvested from the heptane suspension.[8] In the harvesting step, the nanoparticles that have a net spontaneous polarization are separated from nonpolar nanoparticles in a inhomogeneous electric field. By this procedure, two types of suspensions are prepared, one containing mainly ferroelectric nanoparticles (i.e., harvested, tetragonal phase) and the other containing nanoparticles exhibiting no (or only a very weak) dipole moment. Presumably, the nonpolar nanoparticles still consist of the cubic phase, or the spontaneous polarizations of several Weiss domains within the nanoparticles in the tetragonal phase compensate each other. Earlier investigations using a uniform electric field between extended planar electrodes[7,8] have shown that the ground $BaTiO_3$ nanoparticle dispersions do not contain any nanoparticles that have a net charge.

The LC mixtures under investigation consist of the compounds 4′-octyloxy-biphenyl-4-carbonitrile (8OCB) and 4′-octyl-biphenyl-4-carbonitrile (8CB). The two components of these mixtures show a rich meso-morphology, which makes them particularly sensitive as a tool to probe the influence of nanoparticles on the local molecular arrangement. Even in the crystalline state at room temperature, 8OCB can show three polymorphic states.[9,10] Specific interactions between CN groups and biphenyl moieties stabilize the molecular arrangement in metastable long parallelepiped crystals of 8OCB. The unit cell of the more stable needle-shaped crystals of 8OCB contains two paired dimers which are stabilized by hydrogen bonds formed by the CN groups. In the most stable crystalline form, 8OCB molecules are arranged head to head in bilayers where they form an infinite chain. In molecular crystals of the second compound, 8CB, smectic layering is not remarkable.[11] These crystals consist of infinite chains with an antiparallel arrangement of the CN groups of the 8CB molecules. In summary, the solid phases of both 8CB and 8OCB are dominated by dipolar interactions and hydrogen bonding. This is also the case in the mesogenic phases of 8OCB and 8CB: Both substances show the partial bilayer SmA_d phase, where the layers contain dimers. Dimeric fluctuations may even occur in

Received: October 26, 2012
Revised: December 12, 2012
Published: December 17, 2012

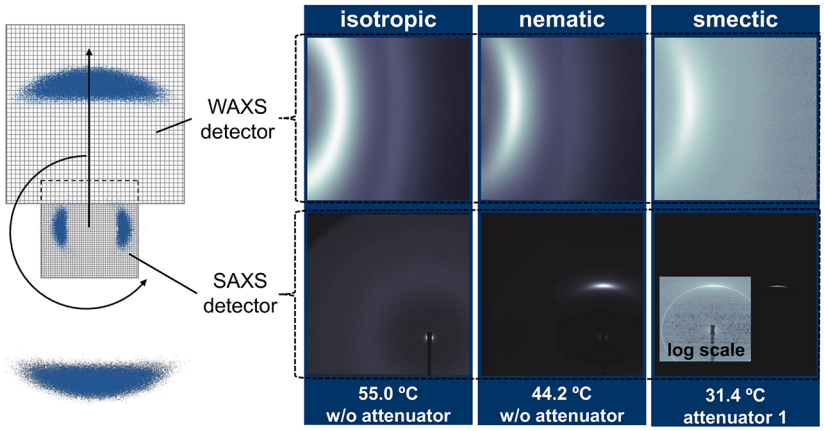

Figure 1. Scheme of the detection setup used to investigate both the characteristic small angle scattering signals and the characteristic wide angle scattering signals of the LC molecules simultaneously with high resolution and characteristic 2D diffraction patterns of isotropic, nematic, and smectic phases.

the nematic (N) phase. Here, a mixture of 8OCB and 8CB near the eutectic composition[12] was doped with either nonpolar or harvested $BaTiO_3$ nanoparticles. The neat mixture shows a rather broad smectic phase ranging from 14 to 43 °C so that the doped LC remained in the smectic phase even when the doping shifted the phase transition temperatures by several degrees.

2. EXPERIMENTAL PROCEDURE

Preparation of the Nanoparticle Dispersions, the LC Mixture, and Doping. Ferroelectric $BaTiO_3$ nanoparticles were dispersed in smectic LCs. First, an initial dispersion of $BaTiO_3$ nanoparticles of ∼15 nm in diameter was prepared by grinding cubic (nonferroelectric) $BaTiO_3$ in a planetary ball mill in the presence of oleic acid as surfactant and heptane as solvent.[6,7] Stress during the grinding process may convert some of the cubic $BaTiO_3$ particles into tetragonal $BaTiO_3$. Consequently, some of the nanoparticles in the initial dispersion will show ferroelectric properties (i.e., possess a dipole moment), while the remainder will not. The ferroelectric nanoparticles were harvested from the initial dispersion by using a strong electric field gradient, as previously reported in the literature.[8] These harvested nanoparticles were then transferred to pure heptane. Both dispersions, of the harvested and the nonpolar nanoparticles, were adjusted to a concentration of 3 mg/mL. These turbid dispersions were kept in glass vessels under continuous stirring with a magnetic stirrer. They showed no flocculation over several weeks.

A mixture of 8OCB [$c_{(8OCB)}$ = 246 mg/g] and 8CB [$c_{(8CB)}$ = 754 mg/g] was prepared in heptane and stirred with a magnetic stirrer in an open glass vessel. The glass vessel along with stirrer was placed in a fume hood, and the solvent was allowed to slowly evaporate at ∼50 °C and ambient pressure until the sample showed mass constancy.

The mixture was prepared by adding a small volume of a nanoparticle dispersion to 0.25 g of the smectic LC. Again, heptane was allowed to evaporate slowly at ∼50 °C and ambient pressure under constant magnetic stirring in a fume hood until the mass of the mixture stopped changing. Doped LCs of two different concentrations (5 and 10 mg/g) were prepared.

Small- and Wide-Angle X-ray Scattering. The neat LCs and nanoparticle dispersions were investigated at beamline ID02 at the European Synchrotron Radiation Facility (ESRF). The SAXS detector (fast-readout, low-noise detector based on the Kodak KAF-4320 CCD detector) and the WAXS detector (AVIEX PCCD-4284, based on the DALSA FTF7040 M CCD-detector) were applied in tandem configuration in order to investigate the characteristic X-ray scattering of the LC molecules in both the SAXS and WAXS ranges simultaneously with high resolution (Figure 1). Both detectors were adjusted to gain overlap of the inspected angular regions: The SAXS detector was adjusted to a sample−detector distance of 1.087 m which yielded a q range of 0.1−5.3 nm^{-1}, and the WAXS detector was adjusted to a sample−detector distance of 0.104 m which yielded a q range of 3.8−45 nm^{-1}.

The samples were filled in 1.5 mm diameter quartz Lindemann capillaries, sealed with epoxy, and placed inside a modified Instec (HCS402) hot stage with a temperature precision of ±0.1 °C and an *in situ* ∼2.5 kG magnetic field produced by a pair of CoSm magnets. The capillaries were centered in the X-ray beam, and the temperature was adjusted to 50 °C where all samples showed an isotropic phase. The samples were then slowly cooled with a rate of 0.2 °C/min in the presence of the magnetic field. The nematic director aligned along the magnetic field, and the structure of the samples was systematically investigated during cooling down to 34 °C. The 2D diffraction patterns were analyzed with the SAXSutilities software package[13] and MATLAB. The scattering curves (intensity vs scattering vector $|q|$, Figure 2) were used to calculate structural parameters.

3. RESULTS

As expected, the phase sequence isotropic (I)-N-SmA_d was observed in all samples. This phase sequence did not fundamentally change upon doping. However, doping caused a decrease of the phase transition temperatures, which was more pronounced in the samples doped with harvested nanoparticles than in the samples doped with nonpolar nanoparticles. In the following, the scattering data is presented and discussed.

The Isotropic to Nematic Transition. The well-known method of Davidson et al.[14] was used to estimate the orientational order parameter S from azimuthal scans (χ-scans) of the diffuse peaks in the WAXS region of the diffraction patterns. The position of this peak is a measure of the average intermolecular separation in the direction perpendicular to the molecular long axis ($d_\perp$).[15] Analysis of

dx.doi.org/10.1021/jp310624c | J. Phys. Chem. B 2013, 117, 937−941

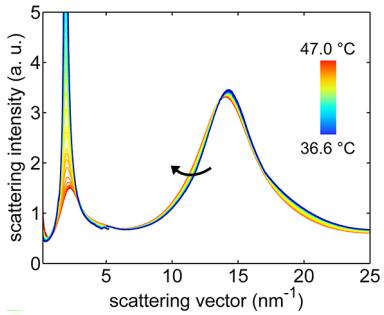

Figure 2. Thermal evolution of the diffracted X-ray intensity vs magnitude of the scattering vector q for the sample doped with a concentration of 10 mg/g of harvested $BaTiO_3$ nanoparticles. In each curve, scattering data recorded with the two different detectors is shown with a small offset near q = 5 nm^{-1}.

χ-scans through this peak yields information on S because the peak-width depends on the degree of orientational order of molecules in the scattering volume. The thermal evolution of the orientational order parameter S is shown in Figure 3. The sample with a doping concentration of 5 mg/g of nonpolar nanoparticles showed the same I → N phase transition temperature T_{NI} as the neat LC. A higher doping concentration of 10 mg/g led to a small decrease of the I → N phase transition temperature T_{NI} by 0.7 °C (Figure 3a). Additionally, this high doping concentration of nonpolar nanoparticles led to a diminished orientational order as compared to the other samples (Figure 3b). A high concentration of nonpolar nanoparticles apparently disturbed the liquid crystalline order by creating orientational disorder and defects to a larger extent. A similar effect was reported for larger particles.[16] Doping with harvested nanoparticles caused a larger decrease of the I → N phase transition temperature (Figure 3a): The low doping concentration of 5 mg/g led to a decrease of 1.5 °C, and the high doping concentration of 10 mg/g led to a decrease of even 4.8 °C. In the nematic phase, S increased with decreasing temperature, as expected. This continuous increase was followed by a noisy region near the impending N → SmA_d phase transition. This noise is very likely due to pretransitional smectic fluctuations,[17,18] which cause fluctuations of the X-ray peak intensity as the size and relative orientation of the correlated regions passing through the X-ray beam fluctuated.

The Nematic to Smectic-A_d Phase Transition. The phase transition N → SmA_d is of second or weakly first order and can preferably be analyzed using SAXS data,[19−21] because the phase transition temperature can be extracted from the peak shape of the SAXS signals.[21] In ref 21, the smectic structure factor was discussed:

$$S(q) \propto \frac{1}{\xi_{\|}(q - q_{center})^2} \quad (1)$$

In a fitting routine, the SAXS signal was deconvolved with a Gaussian of variable width and, subsequently, the smectic correlation length $\xi_{\|}$ was extracted from the deconvolved signals. The thermal evolution of the smectic correlation length is shown in Figure 4. In the present experiments, the detection

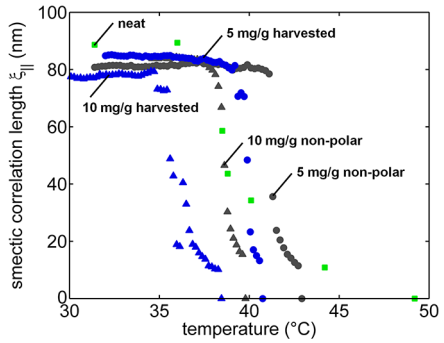

Figure 4. Thermal evolution of the smectic correlation length $\xi_{\|}$ of (■) the neat LC, (●) samples with a doping concentration of 5 mg/g, and (▲) 10 mg/g of nonpolar nanoparticles (gray) and harvested nanoparticles (blue).

limit for smectic correlations was ∼10 nm or ∼10% of the maximum smectic correlation length. This threshold is an appropriate indication of the phase transition temperature. Doping with nonpolar nanoparticles decreases the N → SmA_d phase transition temperature by 1.3 °C (5 mg/g) and 4.4 °C (10 mg/g), respectively. Doping with harvested nanoparticles led to larger decreases of 3.5 °C (5 mg/g) and 6.7 °C (10 mg/g), respectively.

Smectic Layer Spacing. The position of the small angle signal depends on the smectic characteristic distance parallel to the long molecular axis ($d_{\|}$) and can be used to calculate the smectic layer spacing. In the monolayer SmA_1 phase, $d_{\|}$ is comparable to the average molecular length, l. However, the smectic layer spacing is such that $l < d_{\|} < 2l$ in the partially bilayer SmA_d phase.[19−26] The temperature evolution of the smectic layer spacing $d_{\|}$ in 8CB was reported in the literature.[27] It varies between 3.14 and 3.16 nm in the temperature range of 20−33.5 °C. For 8OCB, values of $d_{\|}$ = 2.97 nm (59 °C) and

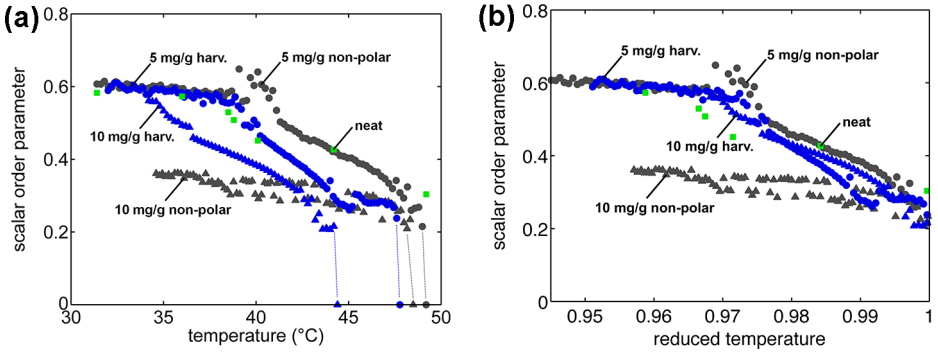

Figure 3. Dependence of the orientational order parameter S on (a) temperature and (b) reduced temperature T/T_{NI}, respectively. (■) The neat LC, (●) samples with a doping concentration of 5 mg/g, and (▲) 10 mg/g of nonpolar nanoparticles (gray) and harvested nanoparticles (blue).

dx.doi.org/10.1021/jp310624c | J. Phys. Chem. B 2013, 117, 937−941

3.15 nm (65 °C) were reported.[28,29] For both compounds, molecular lengths can be estimated (l_{8CB} = 2.24 nm, l_{8OCB} = 2.31 nm).[30] In the present experiments, $d_{\|}$ in the neat mixture of the two compounds is ~3.2 nm. The thermal evolution of $d_{\|}$ for the doped samples is shown in Figure 5. In the isotropic

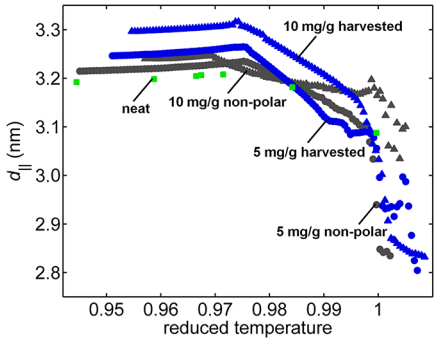

Figure 5. Smectic layer spacing $d_{\|}$ vs reduced temperature. Data of (■) the neat LC, (●) samples with a doping concentration of 5 mg/g, and (▲) 10 mg/g of nonpolar nanoparticles (gray) and harvested nanoparticles (blue).

phase (T_{red} > 1), small values of $d_{\|}$ were observed. Near the I → N phase transition (around T_{red} = 1), an increase in $d_{\|}$ is observed, which can be attributed to nematic order fluctuations. In the N phase (T_{red} < 1), a larger value of $d_{\|}$ was obtained due to the formation of dimers and, to some extent, reduced thermal energy, making the molecules effectively stiffer. Here, $d_{\|}$ corresponds to ~1.5·l. With decreasing temperature, the concentration of dimers in the N phase caused an effective increase in the average molecular length, and thus $d_{\|}$. Below the second order or weakly first order transition to the SmA_d phase, the value of $d_{\|}$ decreased at lower temperatures. This can be explained by an increase in density. Doping with $BaTiO_3$ nanoparticles leads to small increases in $d_{\|}$ in the SmA_d phase as compared to the pure LC. Nonpolar nanoparticles increased $d_{\|}$ by 0.5 and 1.2% in 5 and 10 mg/g concentrations, respectively. Harvested nanoparticles lead to a slightly larger increase in $d_{\|}$ of 1.5 and 3.3% for 5 and 10 mg/g concentrations, respectively.

■ SUMMARY AND CONCLUSIONS

In the present experiments, a wide temperature smectic LC was doped with harvested (polar) and nonpolar $BaTiO_3$ nanoparticles and investigated by X-ray diffraction. The thermal evolution of the nematic order parameter was determined from the wide-angle scattering signal. In addition, the thermal evolution of both the smectic correlation length and the smectic layer spacing was extracted from the small angle scattering signals. The thermal evolution of the smectic correlation length was applied to analyze the N → SmA_d phase transition temperatures.

Harvested nanoparticles are found to change the orientational order parameter to a much lesser extent than nonpolar nanoparticles. Both the I → N and N → SmA_d phase transition temperatures shifted to lower temperatures. This effect is larger for harvested nanoparticles than for nonpolar nanoparticles. In general, the addition of nanoparticles can be considered to be equivalent to addition of impurities which produce random field and confinement effects and create defects. Such effects have previously been investigated in both thermotropic[31−34] and lyotropic[35] liquid crystals. Similar effects were reported in 8CB doped with silica aerogel and small quartz spheres, and poly(ethylene oxide) doped mixtures of a cesium perfluorooctanoate and water. Kurochkin et al.[34] also point out that photoinduced local changes in a homogeneous liquid crystal may be considered as induced impurities, which have a similar effect as nanoparticles. From the present experiments, one can conclude that nonpolar nanoparticles have a more localized effect than polar nanoparticles. The latter probably interact over a larger volume with the LC via their electric field produced in their proximity.

The I → N phase transition temperature and the N → SmA_d phase transition temperature of the mixture of 8CB and 8OCB increases linearly with the molar fraction of 8OCB.[8] Thus, one can speculate that the shifts of the transition temperatures were caused by a change of the molar fraction of 8OCB.

In the present experiments, a small increase of ~0.1 nm in $d_{\|}$ in the SmA_d phase was observed. This cannot be explained by a decrease of the molar fraction of 8OCB, because 8OCB molecules have a (by 0.1 nm) higher length than 8CB molecules. Probably, the effective length of the dimers present in the SmA_d phase is changing with temperature due to changing intermolecular interactions and the degree of overlap between the two dimer molecules.

Doping with harvested $BaTiO_3$ nanoparticles influences not only the phase transition temperatures but also the structure of the mesophases. These changes have only a small effect on the properties of the liquid crystal mixture investigated here. However, doping with harvested nanoparticles may substantially alter other liquid crystals with a very delicate phase sequence, such as smectic LCs with a reentrant nematic phase or smectic blue phases. Maybe doping such self-organized, nanostructured LCs can also show electrically controllable induced changes of the periodicity and enhance the associated electro-optic effects.

■ AUTHOR INFORMATION

Corresponding Author

*E-mail: heinz.kitzerow@uni-paderborn.de. Phone: +49 5251 602156. Fax: +49 5251 604208.

Present Address

[#]Centre of Molecular Materials for Photonics and Electronics, Electrical Engineering Division, Department of Engineering, University of Cambridge, 9 JJ Thomson Avenue, Cambridge CB3 0FA, United Kingdom.

Notes

The authors declare no competing financial interest.

■ ACKNOWLEDGMENTS

The authors would like to express their gratitude to Theyencheri Narayanan (ESRF) for his excellent support and valuable discussions. Financial support by the German Research Foundation (KI 411/14 and GRK 1464), the European Science Foundation (EUROCORES, SONS II, "Self-organized nanostructures"), the European Synchrotron Radiation Facility (ESRF), and (S.K.) the US Department of Energy, Office of Science, Basic Energy Sciences grant DE-SC0001412 is gratefully acknowledged.

■ REFERENCES

(1) Cook, G.; Reshetnyak, V. Yu.; Ziolo, R. F.; Basun, S. A.; Banerjee, P. P.; Evans, D. R. *Opt. Express* **2010**, *18*, 17339−17345.

(2) Buchnev, O.; Dyadyusha, A.; Kaczmarek, M.; Reshetnyak, V.; Reznikov, Y. *J. Opt. Soc. Am. B* **2007**, *24*, 1512−1516.
(3) Cook, G.; Glushchenko, A.; Reshetnyak, V.; Griffith, A. T.; Saleh, M. A.; Evans, D. R. *Opt. Express* **2008**, *16*, 4015−4022.
(4) Glushchenko, A.; Cheon, C. I.; West, J.; Lic, F.; Büyüktanir, E.; Reznikov, V.; Buchnev, A. *Mol. Cryst. Liq. Cryst.* **2006**, *453*, 227−237.
(5) Li, F.; Buchnev, O.; Cheon, C.-I.; Glushchenko, A.; Reshetnyak, V.; Reznikov, Y.; Sluckin, T. J.; West, J. L. *Phys. Rev. Lett.* **2006**, *97*, 147801; **2007**, *99*, 219901.
(6) Atkuri, H.; Cook, G.; Evans, D. R.; Cheon, C.-I.; Glushchenko, A.; Reshetnyak, V.; Reznikov, Y.; West, J.; Zhang, K. *J. Opt. A: Pure Appl. Opt.* **2009**, *11*, 024006.
(7) Basun, S. A.; Cook, G.; Reshetnyak, V. Yu.; Glushchenko, A. V.; Evans, D. R. *Phys. Rev. B* **2011**, *84*, 024105.
(8) Cook, G.; Barnes, J. L.; Basunm, S. A.; Evans, D. R.; Ziolo, R. F.; Ponce, A.; Reshetnyak, V. Y.; Glushchenko, A.; Banerjee, P. P. *J. Appl. Phys.* **2010**, *108*, 064309.
(9) Hori, K.; Kurosaki, M.; Wu, H.; Itoh, K. *Acta Crystallogr., Sect. C* **1996**, *52*, 1751−1754.
(10) Davey, R. J.; Gillon, A. L.; Quayle, M. J.; Rashad, O. *Acta Crystallogr., Sect. C* **2005**, *61*, o143−o144.
(11) Kuribayashi, M.; Hori, K. *Acta Crystallogr., Sect. C* **1998**, *C54*, 1475−1477.
(12) Sied, M. B.; LóPez, D. O.; Tamarit, J. L.; Barrio, M. *Liq. Cryst.* **2002**, *29*, 57−66.
(13) Sztucki, M.; Narayanan, T. *J. Appl. Crystallogr.* **2007**, *40*, s459−s462.
(14) Davidson, P.; Petermann, D.; Levelut, A. M. *J. Phys. II (France)* **1995**, *5*, 113−131.
(15) McMillan, W. L. *Phys. Rev. A* **1971**, *4*, 1238−1246.
(16) Gupta, M.; Satpathy, I.; Roy, A.; Pratibah, R. *J. Colloid Interface Sci.* **2010**, *352*, 292−298.
(17) Chen, L.; Brock, J. D.; Huang, J.; Kumar, S. *Phys. Rev. Lett.* **1991**, *67*, 2037−2040.
(18) Primak, A.; Fisch, M.; Kumar, S. *Phys. Rev. Lett.* **2002**, *88*, 035701.
(19) McMillan, W. L. *Phys. Rev. A* **1972**, *6*, 936−947.
(20) McMillan, W. L. *Phys. Rev. A* **1973**, *7*, 1673−1678.
(21) Primak, A.; Fisch, M.; Kumar, S. *Phys. Rev. E* **2002**, *66*, 051707.
(22) Pershan, P. S. *Structure of liquid crystal phases*; World Scientific Lecture Notes in Physics *23*; World Scientific Publ.: Singapore, 1998.
(23) Patel, P.; Kumar, S.; Ukleja, P. *Liq. Cryst.* **1994**, *16*, 351−371.
(24) Patel, P.; Keast, S. S.; Neubert, M. E.; Kumar, S. *Phys. Rev. Lett.* **1992**, *69*, 301−304.
(25) Chan, K. K.; Pershan, P. S.; Sorensen, L. B.; Hardouin, F. *Phys. Rev. A* **1986**, *34*, 1420−1424.
(26) Cladis, P. E. *Liq. Cryst.* **1998**, *24*, 15−19.
(27) Krentsel (Lobko), T. A.; Lavrentovich, O. D.; Kumar, S. *Mol. Cryst. Liq. Cryst.* **1997**, *304*, 463−69.
(28) Lydon, J. E.; Coakley, C. J. *J. Phys. Colloq.* **1975**, *36*, C1−45.
(29) Madsen, A.; Struth, B.; Grübel, G. *Physica B* **2003**, *336*, 216−221.
(30) Cladis, P. E.; Bogardus, R. K.; Aadsen, D. *Phys. Rev. A* **1978**, *18*, 2292−2306.
(31) Iannacchione, G. S. *Fluid Phase Equilib.* **2004**, *222*, 177−187.
(32) Bellini, T.; Radzihovsky, L.; Toner, J.; Clark, N. A. *Science* **2001**, *294*, 1074−1079.
(33) Zhou, B.; Iannacchione, G. S.; Garland, C. W.; Bellini, T. *Phys. Rev. E* **1997**, *55*, 2962−2968.
(34) Kurochkin, O.; Atkuri, H.; Buchnev, O.; Glushchenko, A.; Grabar, O.; Karapinar, R.; Reshetnyak, V.; West, J.; Reznikov, Yu. *Condens. Matter Phys.* **2010**, *13* (3), 33701.
(35) Kuzma, M. R.; Wedler, W.; Saupe, A.; Shin, S.; Kumar, S. *Phys. Rev. Lett.* **1992**, *68*, 3436−3439.